Evolution of bridge frequencies and modes of vibration during truck passage

Cantero, D., Hester, D., & Brownjohn, J. (2017). Evolution of bridge frequencies and modes of vibration during truck passage. *Engineering Structures*, *152*, 452-464. https://doi.org/10.1016/j.engstruct.2017.09.039

Published in:
Engineering Structures

Document Version:
Peer reviewed version

Queen's University Belfast - Research Portal:
Link to publication record in Queen's University Belfast Research Portal

Publisher rights
Copyright 2017 Elsevier.
This manuscript is distributed under a Creative Commons Attribution-NonCommercial-NoDerivs License (https://creativecommons.org/licenses/by-nc-nd/4.0/), which permits distribution and reproduction for non-commercial purposes, provided the author and source are cited.

General rights
Copyright for the publications made accessible via the Queen's University Belfast Research Portal is retained by the author(s) and / or other copyright owners and it is a condition of accessing these publications that users recognise and abide by the legal requirements associated with these rights.

Take down policy
The Research Portal is Queen's institutional repository that provides access to Queen's research output. Every effort has been made to ensure that content in the Research Portal does not infringe any person's rights, or applicable UK laws. If you discover content in the Research Portal that you believe breaches copyright or violates any law, please contact openaccess@qub.ac.uk.

Open Access
This research has been made openly available by Queen's academics and its Open Research team. We would love to hear how access to this research benefits you. – Share your feedback with us: http://go.qub.ac.uk/oa-feedback

Download date:18. Apr. 2024

Title

Evolution of bridge frequencies and modes of vibration during truck passage

Authors
Daniel Cantero (1)
David Hester (2)
James Brownjohn (3)

Affiliations
1) Department of Structural Engineering, Norwegian University of Science & Technology NTNU, Trondheim, Norway
2) School of Natural and Built Environment, Queen’s University Belfast, Northern Ireland.
3) Vibration Engineering Section, University of Exeter, Kay Building North Park Road, EX4 4QF

Abstract

This paper reports an experimental campaign that aims at measuring the evolution of bridge modal properties during the passage of a vehicle. It investigates not only frequency shifts due to various vehicle positions, but also changes in the shape of the modes of vibration. Two different bridges were instrumented and loaded by traversing trucks or trucks momentarily stationed on the bridge. The measurements were analysed by means of an output-only technique and a novel use of the continuous wavelet transform, which is presented here for the first time. The analysis reveals the presence of additional frequencies, significant shifts in frequencies and changes in the modes of vibration These phenomena are theoretically investigated with the support of a simplified numerical model. This paper offers an interpretation of vehicle-bridge interaction of two particular case studies. The results clearly show that the modal properties of the vehicle and bridge do change with varying vehicle position.

Keywords

vehicle-bridge interaction, modal analysis, nonstationary, wavelet

1. Introduction

It is a well-known fact that the modal properties of two separate mechanical systems change when both systems interact. The coupled arrangement might have significantly different natural frequencies and modes of vibrations, compared to the uncoupled systems [1]. This is also acknowledged in bridge engineering to some extent, when investigating vehicles crossing the structure, i.e. it is understood that natural frequencies of a bridge change when heavy (massive) traffic traverses it.

As pointed out by Frýba [2] the fundamental frequency of a loaded beam depends not only on the magnitude of the mass on the deck but also on the position of the mass. A key factor in the scale of frequency variation that occurs for different mass positions is the ratio between the vehicle and bridge masses, with higher mass ratios producing larger shifts in the bridge frequency. Despite the general acceptance that such frequency shifts will occur, this is a problem not well studied in bridge engineering literature [3]. However, there have been some recent studies, for example [4] describes changes in the fundamental frequency of a railway bridge during passage of a train and provides an approximate formula to calculate changing bridge frequency. Yang et al. [3] study the variation of both vehicle and bridge frequencies and present a closed-form expression for a simply supported bridge considering only the first mode of vibration. Cantero & OBrien [5] investigate numerically the effect of different mass ratios and frequency ratios on the changes in system frequencies, where frequency ratio (FR) = vehicle frequency / bridge frequency and mass ratio (MR) =vehicle mass / bridge mass. The numerical analyses of coupled vehicle-bridge models in [5, 6] show that for certain mass and frequency ratios it is possible to achieve positive frequency shifts in the fundamental frequency of the bridge. There exist only a limited number of studies that investigate this problem either experimentally, or in real operational bridges. For instance, in [7] the authors use a variety of output-only techniques with the response of a scaled model and are able to obtain clear frequency evolution diagrams for the case of large mass ratios. Also [6] performs a controlled laboratory experiment obtaining frequency shifts that validate an approximate closed-form solution of the frequency shift. The study in [8] investigates how a parked vehicle on an operational bridge affects its fundamental frequency, reporting frequency reductions of 5.4%. More recently, [9] explores the non-stationary nature of a 5-span bridge traversed by a truck, using alternative time-frequency tools, with limited success. Frequency is not the only modal property changing with load and its position; for instance [10] used numerical simulation to show that damping of a pedestrian bridge also changes according to number and location of pedestrians. That said, the majority of the limited papers available on the topic focus only on tracking frequency changes and do not evaluate the effect of load on the associated mode shapes.

Although a small number of authors have used numerical models to study the problem of frequency variation with load position, to date, no experimental investigation on full scale bridges has been presented. Such a study is the main contribution of this paper. Two seperate experiments were carried out, each using a different test truck on different instrumented bridges. Bridge A is a three-span continuous structure monitored while a truck traverses it at a constant speed. The measurements from Bridge A provide only weak evidence of the evolution of the modal properties and hence it constitutes only a first attempt. A second experiment is reported on Bridge B, which is a single span bridge. For the experiment on Bridge B, a truck stops at certain locations on the bridge. The free vibration measurements of the bridge accelerations, right after the vehicle stops, allows for the precise extraction of the modal parameters of the coupled system. This is repeated for various vehicle stopping positions to obtain the variation of the modal properties with respect to vehicle position. It is important to note that the variation in modal properties reported here are specific to the two case studies investigated; since these variations strongly depend on the particular vehicle and bridge.

Over the course of the investigation, it is shown that a vehicle being present on the bridge results in a coupled system, such that modal analysis results cannot be interpreted as two separate systems (bridge and truck). The vehicle-bridge interaction is a non-stationary problem where the modal parameters change with vehicle location. In general, the ideas and results presented here are of interest to engineers and researchers involved in any vehicle-bridge interaction study. However, the findings reported here have particular consequences for the current research thread on extracting bridge modal properties from passing instrumented vehicles, e.g. [11-13]. In general, these publications acknowledge that there is vehicle-bridge coupling, but fail to consider the changes in modal properties with vehicle position. In these papers modal analysis techniques are often applied to the full length of the signal obtained during vehicle passage. However, attempting to analyse what is in effect a non-stationary signal with conventional modal analysis techniques developed for stationary signals will necessarily result in unreliable modal properties.

As well as demonstrating that the bridge acceleration signal recorded during the passage of a truck is non-stationary, this paper provides advice and insight on a number of related issues. First, a modified and novel approach for performing the Continuous Wavelet Transform (CWT) is presented, and is shown to be an effective signal processing technique to visualise variations in system frequencies. Next, the source of the additional frequency peak in the spectra of the forced (i.e. loaded) bridge acceleration signal is investigated. This is carried out using a relatively simple but insightful numerical model, and experimental data from Bridges A and B. Moreover, this paper shows for the first time that not only do the natural frequencies evolve during traffic passage, but that the shapes of the associated modes of vibration also evolve. For every vehicle location, the vehicle-bridge system features distinctly different modes. This is supported by a theoretical analysis of the problem, and carefully extracted experimental results. However, it should be noted that this paper only reports findings on the first longitudinal mode of the bridge, no torsional or higher modes are investigated.

The remainder of this paper has four primary sections. Section 2 provides a theoretical background on the numerical model, modal analysis, and signal processing techniques used in this study. Section 3 describes an experimental test where a truck was driven across a 3-span bridge. Additional frequencies were observed in the spectra of the recorded bridge response. A numerical model is used to postulate the origin of the additional frequency peak. However, to experimentally confirm the validity of the model predictions it was necessary to redo the experiment using a revised procedure where the truck would stop at a series of discrete locations on a bridge. The outcome of the revised experiment is reported in Section 4.

2. Methods

This section provides the reader a brief overview of the tools used throughout this study. Section 2.1 describes the numerical model that helps explain non-intuitive changes in modal properties observed in the experiments. Section 2.2 provides references on the modal analysis procedures employed to analyse the measured acceleration signals. Finally, Section 2.3 describes a modified form of wavelet analysis that is used to visualise variations in the system frequencies for the non-stationary acceleration signals recorded on site.

2.1 Numerical model

The coupled vehicle-bridge model was programmed in Matlab [14] and a pictorial representation of the numerical model is shown in Fig. 1. The truck is simulated as a sprung mass *m* supported on a spring *k*, where the spring represents the suspension of the vehicle. The bridge is simulated using a finite element beam model where each beam element has 4 degrees of freedom, namely a rotation and a vertical translation at each end of the element. Elemental matrices for this kind of element can be found in the literature, e.g. [15]. The beam is defined by its span *L*, section area *A*, modulus of elasticity *E*, second moment of area *I* and mass per unit length ρ. The location of the vehicle is defined by the distance from the left support (x) and in the simulations the vehicle can be positioned anywhere on the beam ($0 \leq x \leq L$). The coupling between both systems, i.e. bridge and vehicle, can be written in terms of the beam element shape functions and the relative position of the vehicle within that element [16]. However, defining a sufficiently dense mesh that has a node exactly at the location of the vehicle reduces the complexity of the procedure. In that case the matrices of both systems are assembled diagonally, and the coupling terms are off-diagonal negative stiffness values that link together the appropriate degrees of freedom. As two different bridges will be modelled, (each with different boundary conditions), for now the boundary conditions of the model are indicated with question marks in Fig. 1. Models of this type have previously been presented in the literature [17].

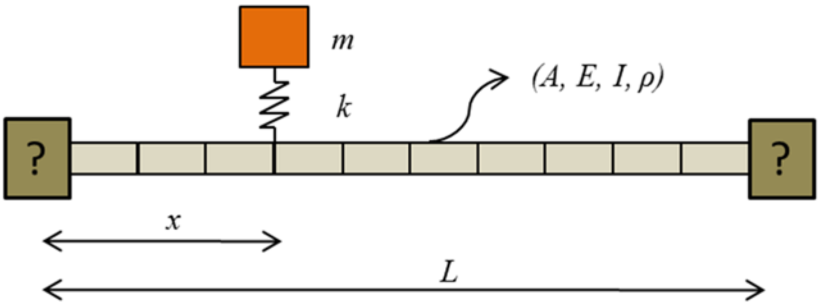

Fig. 1: Coupled Vehicle-Bridge finite element model

Fundamentally, the purpose of this model is to allow the vehicle to be moved incrementally across the bridge and to track how the bridge frequency changes with the position of the vehicle. For a given vehicle position, the bridge frequencies and associated modes of vibration can be determined using an eigenvalue analysis. Simulating a multi-axle truck as a single degree of freedom sprung mass is a simplification, and for some applications it would be an over simplification. However, it is shown later that for the purpose of this study, where the primary interest is in explaining the evolution of frequency with respect to truck position, the model is effective. Initially values for area (*A)*, second moment of area (*I)* and mass per unit length (*ρ)* were determined from the available bridge drawings. For the Young's Modulus (*E*), standard values for steel and concrete of 2x10^{11} N/m^{2} and 2x10^{10} N/m^{2} respectively were used. After getting an initial estimate of bridge frequencies from the model, the bridge properties (in the model) are revised so that the fundamental bridge frequency of the model matches the free vibration frequency observed on site, this is further described in Sections 3 and 4. For the vehicle, the spring stiffness (*k*) is adjusted so that the vehicle frequency in the model matches the vehicle frequency inferred from the acceleration measurements recorded experimentally when the truck was traversing the real bridge. Table 1 gives a summary of relevant information about the vehicle and bridge properties used in this paper. It can be seen in Table 1 that the vehicle properties postulated for the test vehicles give body bounce frequencies that are in accordance with typical values for heavy vehicles (1 Hz to 4 Hz) as shown in [18].

Table 1: Vehicle and bridge properties

		Test on Bridge A	Test on Bridge B
Bridge	Type	3-span continuous	1-span
	Spans (m)	18+31+18	36
	f_b (Hz)	3.50	3.13
Vehicle	Mass (kg)	26 000	32 000
	f_v (Hz)	2.80	2.60
	Number of axles	3	4
	Axle distances (m)	1.4+4.1	2.0+3.5+1.4
	Velocity (m/s)	3.63	-

2.2 Bridge modal analysis

The Introduction provided an overview of literature dealing with variation in bridge frequency with respect to variation in mass distribution. It was also highlighted that previous studies have not looked at how the mode shapes associated with these frequencies change with respect to variation in mass distribution. To address this limitation this study attempts to experimentally capture the mode shape associated with a particular truck position. This is achieved using output-only modal analysis methods, i.e. no information on the excitation is measured. Due to the size/mass of road bridges, output-only methods are often the only logistically feasible approach to extract modal parameters, because using shakers or impact hammers to excite the structure is often not practical. Specific details on the theory/ mathematics underlying output-only modal analysis are not provided here as the topic has been extensively covered in other publications such as [19]. The particular method used in this paper is Frequency Domain Decomposition (FDD) and details on this method are given in [20].

2.3 Wavelets

To be able to accurately visualise the variation in frequency with respect to time, some time-frequency representation of the recorded signals is necessary. There are a number of time-frequency analysis methods available, e.g. Short Time Fourier Transform, Hilbert-Huang transform and Wavelet transform. Within each of these methods, different options in their implementation can significantly change the time-frequency plots that are output. All time-frequency analysis methods involve a trade-off in resolution, i.e. high resolution in the frequency domain typically means poor resolution in the time domain, and vice versa. Ultimately, it is up to the analyst to identify which method best achieves their objective. In this paper, the objective of the time-frequency analysis is to visualise how the bridge frequency changes as a truck traverses the bridge.

In essence, the CWT compares the wavelet bases (a wave-form of finite length) to the analysed signal and gives a wavelet coefficient, so that the better the match, the larger the coefficient. This wavelet is then shifted in time to cover the whole length of the signal, resulting in a vector of wavelet coefficients. The wavelet is then scaled (i.e. stretched) and the process is repeated. For each scale used in the analysis a vector of wavelet coefficients results. Scale can be regarded as inversely proportional to frequency and thus can be transformed approximately to frequency, or more specifically pseudo-frequency. The result of CWT analysis is a plot of wavelet coefficients in the time-frequency plane that are proportional to the energy of the signal. For additional information on wavelets and to find a full mathematical description further details are provided by other authors [21,22].

When using the CWT, several wavelet basis functions are available, e.g. Morlet, Gaussian, Mexican hat. The results from the CWT are significantly affected by the wavelet basis used in the analysis so it is paramount to choose an appropriate basis. Knowing which wavelet basis will give the best results for a given application is not always obvious, and often there is a degree of trial and error involved. However, [23] showed that the Modified Littlewood-Paley (MLP) wavelet basis was effective when analysing the acceleration signals of bridges subject to vehicle loading, and therefore this is the wavelet basis used in this study.

In addition, this paper proposes a non-conventional normalisation step that proves very effective when analysing bridge signals that contain a mixture of free and forced vibration. Using a conventional CWT to analyse a bridge signal that has both free and forced vibration can be difficult. The forced vibration part of the signal has the largest amplitude, and as a result this will dominate the resulting CWT plot. This makes it very difficult to track the frequency evolution between the free and forced parts of the signal because the frequency from the free vibration part will be practically invisible. The novel procedure adopted here gets around this problem by normalising the wavelet coefficients at each time instant and is presented schematically in Fig. 2.

A signal with linearly increasing frequency and linearly decreasing amplitude is analysed with a conventional CWT and the result is shown in Fig. 2(a). The plot represents a 3D wavelet surface as a 2D ‘contour’ plot where the magnitude of the wavelet coefficients are conveyed using colour, with darker colours implying large values of wavelet coefficient. The non-stationarity property and decreasing amplitude of this numerically generated signal can clearly be appreciated in the plot. Unfortunately, from the point of view of frequency tracking, the large amplitudes in the early part of the signal are resulting in high wavelet coefficients that are in a sense dominating the plot and making it difficult to see the frequency content in the latter part of the signal. However, if one is prepared to sacrifice information relating to amplitude, which for the purpose of this paper we are not concerned with, then this representation can be improved. The first step is to fit an envelope to the wavelet coefficients for a given scale and to accept this curve as the representative result from the CWT. An example of this curve fitting is shown in Fig. 2(b). The blue plot in Fig. 2(b) shows the wavelet coefficients at a particular scale, the red curve has been fitted to the blue plot. If a similar curve is fitted at every scale, and then if all the ‘fitted’ curves are plotted in 2D, the plot shown in Fig. 2(c) results. The second step is to normalise each wavelet coefficient at a given time instant by the total energy content for that time instant. The result of applying this normalisation is shown in Fig. 2(d). The consequence of this normalization is that it gives the same importance to the frequency of small amplitude vibrations as it does to the frequency of large amplitude vibrations. The usefulness of this normalization will become clear when studying the measured accelerations in Sections 3 and 4 below. Obviously, the substitution by the envelope curve and then later application of normalization comes with a cost. The final map of wavelet coefficients cannot be used for signal reconstruction. However, for visualization purposes these two operations greatly improve the final result from the CWT.

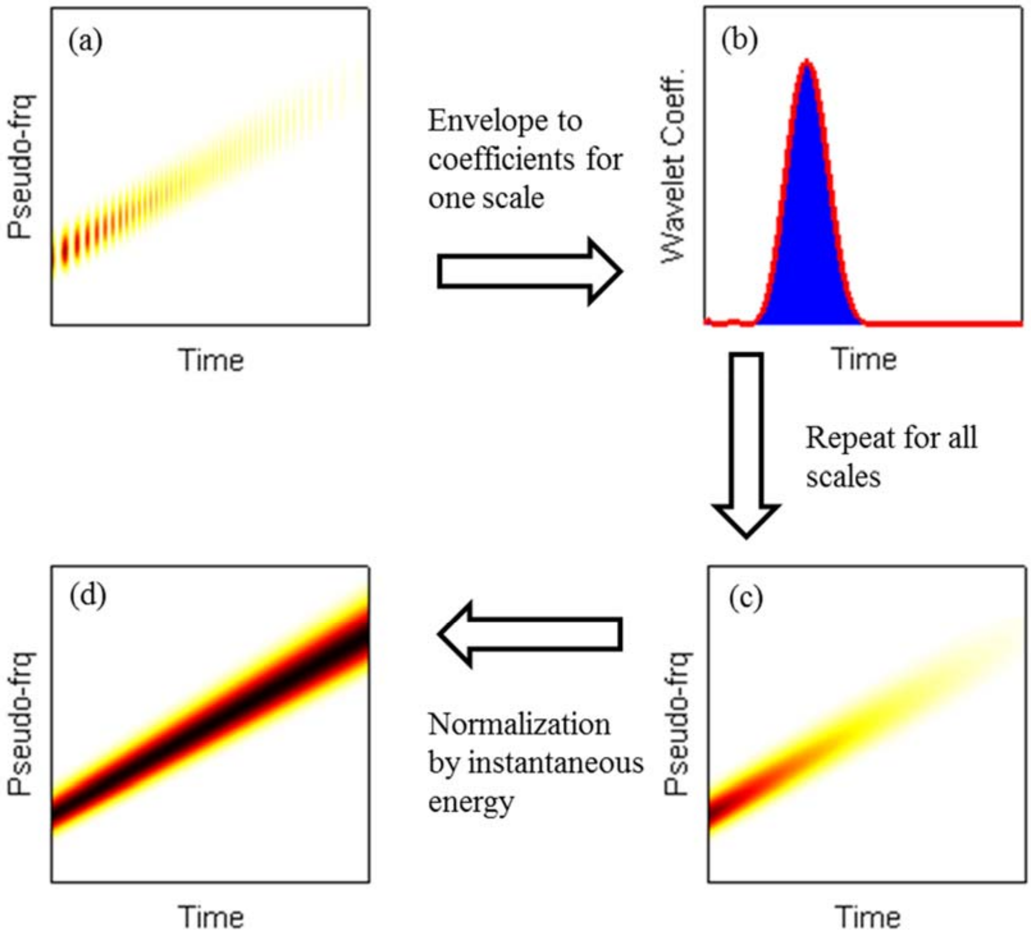

Fig. 2: Enhancement of energy map from CWT analysis

3. Experimental study of Bridge A and moving truck

This section describes the first experimental investigation carried out on a 3-span road bridge. A truck is driven over the bridge and the bridge acceleration is recorded at a number of locations. This acceleration data is subsequently analysed to examine how the modal parameters of the bridge change as the truck crosses the bridge. Section 3.1 describes the bridge and experiment setup used. Section 3.2 presents the results of modal analysis carried out on free and forced vibration data. Finally, Section 3.3 puts forward a theoretical model to explain the behaviour observed in Section 3.2. Note that this experiment on Bridge A is only the first attempt to study the evolution of modal properties during vehicle passage and a plausible explanation is provided based only on weak evidence. A second experiment that provides stronger evidences is performed on a different bridge and is reported in Section 4.

3.1 Bridge and instrumentation description

The bridge used in the experiment is shown in Fig. 3(a). It is a 3-span bridge carrying a minor road (4 m wide) over a dual carriageway. The deck consists of 2 steel girders supporting a concrete deck. The centre span is 31 m and each of the side spans are 18 m. There were two primary reasons for selecting this bridge. Firstly, the bridge deck is relatively light, narrow carriageway and primary members are steel. This is advantageous because a high (vehicle-bridge) mass ratio should lead to larger changes in modal properties. The second reason for selecting this bridge is that the traffic volumes on the bridge are very light, which made it logistically feasible to carry out the test. The vehicle used in the test is a 3-axle truck with a total mass of 26 tonnes, shown in Fig. 3(b). The truck crossed the bridge twice (once in each direction) at a crawling speed of approximately 13 km/h (3.63 m/s). Such a low speed effectively reduces the dynamic effects associated with (i) road profile unevenness, (ii) loading frequencies due to the vehicle's axle spacing and (iii) shifting of bridge frequencies [24]. Despite the low speed the truck still provides sufficient excitation to the system.

Fig. 3: (a) Bridge A elevation (3-span bridge); (b) Truck used in experiment

Fig. 4 shows a plan view of the bridge deck. The position of the piers is indicated using dashed lines and for convenience the spans are labelled as spans 1-3. The bridge has a 4 m wide carriageway with 0.5 m wide footways on either side. Due to the impossibility of road closure, the instrumentation had to be installed on the footway and it was installed as close as possible to centre of the main beams. The location of the six accelerometers (A-F) used in the test are indicated in Fig. 4. One accelerometer was placed at mid-span of each of the three spans on both sides of the bridge. The accelerometers used were tri-axial Micro-Electro Mechanical System (MEMS) accelerometers scanning at 128 Hz.

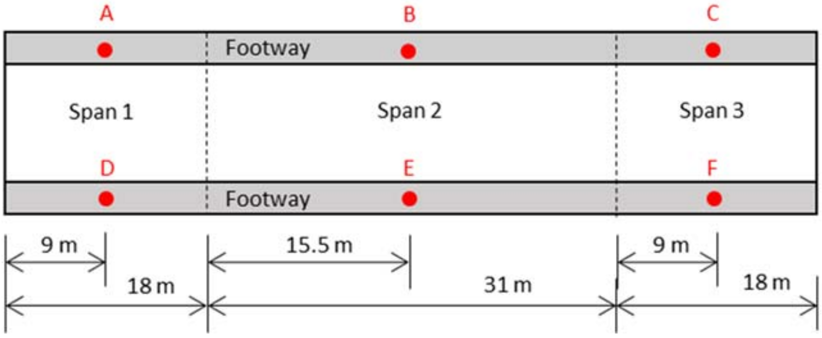

Fig. 4: Plan view and accelerometer layout on Bridge A.

3.2 Modal analysis of free and forced vibration data

The first step in analysing the data is to perform modal analysis on the free vibration data, i.e. no truck on the bridge. The FDD modal analysis approach described in Section 2.2 is used to analyse the free vibration data. Singular Value Decomposition (SVD) of the Power Spectral Density matrix is plotted in Fig. 5(a) where a clear peak is visible at 3.5 Hz indicating the likely presence of a mode. Note that the poor frequency resolution is due to the short duration of analysed signal. The associated mode of vibration is extracted and presented in Fig. 5(b). The square data markers represent the bridge supports, i.e. the modal amplitude at these locations is assumed zero. The circular data markers (from left to right) indicate the modal amplitudes at sensor locations A, B and C, see Fig. 4. If the modal ordinates for sensor locations D, E and F are plotted the same mode shape is apparent. Thus it is clear that the mode at 3.5 Hz is the first bending mode. This result is consistently obtained for various different free vibration measurements.

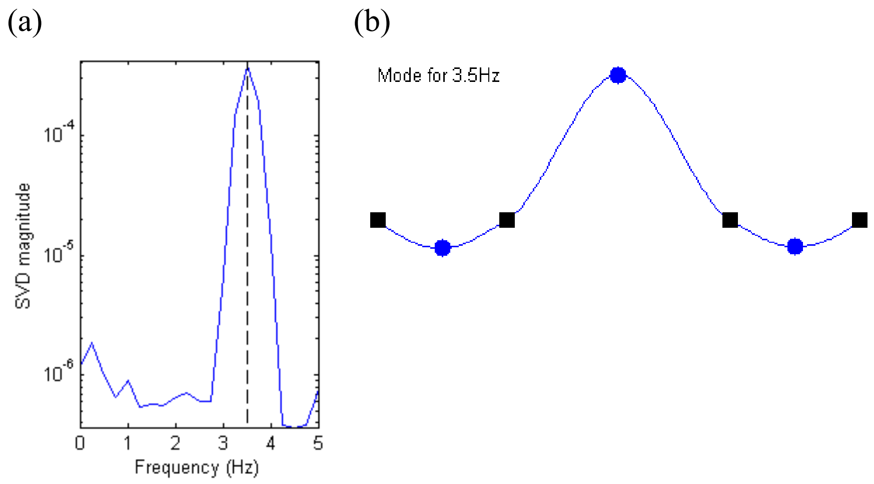

Fig. 5: Modal analysis of signals during free vibration of Bridge A; (a) Singular Value Decomposition magnitude; (b) Extracted fundamental mode

Once the free vibration data was analysed the next step was to analyse the forced vibration response, i.e. the acceleration recorded while the truck was on the bridge. The results of analysing the forced vibration data is presented in Fig. 6. The analysis procedures used are the same as those used to generate the plots in Fig. 5. However, there are in this case, some noticeable differences in the results. The SVD analysis in Fig. 6(a) identifies the presence of two distinct peaks at 2.63 Hz and 3.63 Hz respectively, but the fundamental bridge mode at 3.5 Hz identified in Fig. 5 is no longer evident. The mode shapes associated with the two frequency peaks are shown in Fig. 6(b).

Starting with the mode shape for the 3.63 Hz mode, it is noticeable that it is very similar in shape to the mode shown in Fig. 5(b), so it is reasonable to assume that this is the same mode. However, the presence of the truck has changed the frequency of the mode slightly. It is interesting to note that the fundamental frequency of the bridge has increased. Intuitively one would expect a slight reduction in the frequency because the truck is adding mass to the deck. Moving on to the mode identified at 2.63 Hz, its origins are less clear. One possibility is that perhaps the loading frequency produced an excitation in the region of 2.63 Hz. For this truck three possible axle spacings need to be considered, namely 1.4 m, 4.1 m and 5.5 m, which are the distances from axle-1 to axle-2, axle-2 to axle-3, and axle-1 to axle-3 respectively. For a traversing speed 3.63 m/s the possible loading frequencies are 0.38 Hz, 1.13 Hz and 1.52 Hz. Another possibility is that the shift in bridge frequency is due to the driving velocity of the vehicle, as discussed in Yang et al. [24]. This shift in frequency is directly proportional to the vehicle speed and inversely proportional to double the bridge span. Due to the low speed of the traversing vehicle, only shifts of ±0.03 Hz in the bridge fundamental frequency can be expected. Therefore, neither the vehicle loading frequency nor the frequency shift due to driving velocity explain the frequency peak at 2.63 Hz.

Obviously, the origins of the 2.63 Hz frequency is likely to be related to the vehicle's presence, and it is reasonable to consider that the 2.63 Hz may be the vehicle frequency however, it is difficult to be definitive just on the evidence of Fig. 6. Interestingly the mode shape associated with the 2.63 Hz peak is practically a duplicate of the fundamental bridge mode identified in Fig. 5(b). Therefore, to get a better theoretical understanding of why the presence of a truck is; (i) causing a slight increase in the frequency of the fundamental mode and (ii) resulting in the appearance of a new mode, the vehicle-bridge model described in Section 2.1 is used in the next section to calculate the system frequencies for a series of different vehicle positions.

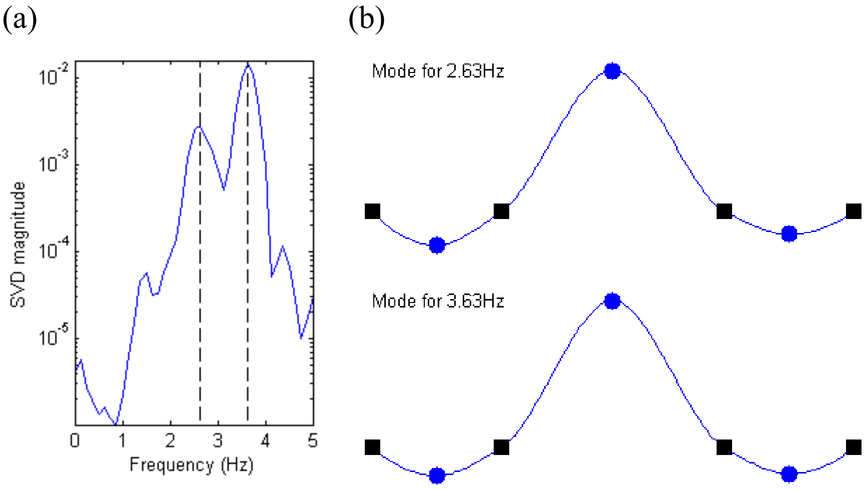

Fig. 6: Modal analysis of signals during forced vibration of Bridge A; (a) Singular Value Decomposition magnitude; (b) Extracted first and second modes

3.3 Theoretical model of observed behaviour

In an effort to better understand the frequencies observed in Fig. 6 the vehicle-bridge model described in Section 2.1 is used here to position the vehicle model at a series of discrete points along the length of the beam and to examine how the frequencies of the system (vehicle and bridge) are affected. The bridge is modelled as a 3-span continuous beam with restrained vertical displacements at the ends and intermediate locations, which represent the support conditions at the abutments and over the piers. The bridge properties in the model are revised so that the fundamental frequency in the model is 3.5 Hz and the properties of the vehicle model have been adjusted to get a vehicle frequency of 2.8 Hz. The total mass of the vehicle in the model is 26000 kg. Although the exact frequency of the vehicle was not measured on site, based on the experimental observations in the previous section, and the information in the literature [18], a vehicle frequency of 2.8 Hz seems reasonable. It should be noted that the purpose of this model is not to exactly simulate the vehicle crossing event recorded experimentally. Instead, the purpose is to examine what happens to the bridge and vehicle frequencies if the sprung mass is placed at a series of discrete points along the length of the beam. This is achieved by positioning the sprung mass at a given point on the bridge and performing an eigenvalue analysis the system matrices of the coupled model system to identify the system frequencies for that vehicle position. Then the vehicle is consecutively moved to the next point on the bridge and the system frequencies for each new position are calculated. As the vehicle-bridge system is coupled, technically these frequencies should be termed the 'first system frequency', 'second system frequency', etc. However, for convention in the following discussion they are also referred to as 'vehicle' and 'bridge' frequencies.

The evolution of the system frequencies for various vehicle positions is presented in Fig. 7. The horizontal axis in Fig. 7 shows the position of the vehicle relative to the left support as a percentage of the total bridge length L. So when the vehicle is exactly over the left support its position is 0% of L, when it is half way across its position is 50% of L, and when it is exactly over the right support its position is 100% of L. The two dashed vertical lines in the figure at 26% and 73% indicate the position of the two piers. The ordinates in Fig. 7 are frequency values. The two horizontal lines at 3.5 Hz and 2.8 Hz represent the vehicle and bridge frequencies in isolation, i.e. in the absence of any interaction between them.

The lower solid line in Fig. 7 shows the variation in the vehicle frequency as the vehicle is at various positions along the length of the bridge. Tracing this plot from left to right, it can be seen that when the vehicle is positioned over the left support its frequency (2.8 Hz) remains unchanged. However, when the vehicle is positioned toward the centre of span 1 ($x \approx 13\%$) the vehicle frequency drops below 2.8 Hz. Then, as the vehicle is positioned at the first pier ($x \approx 26\%$), the vehicle frequency goes back up to 2.8 Hz. As the vehicle is incrementally moved toward the centre of span 2 the vehicle frequency shows a steady reduction in frequency to a minimum value of approximately 2.4 Hz at the mid-span of span 2 ($x \approx 50\%$).

As the position of the vehicle continues toward pier 2 the vehicle frequency shows a gradual increase and it recovers completely to 2.8 Hz when the vehicle is over pier 2. A similar reduction in vehicle frequency is evident when the vehicle is positioned in the centre of span 3. If the vehicle is thought of in isolation, i.e. if it is visualised as a mass supported on a spring, this pattern is difficult to understand. However, if, for the crossing event, the vehicle is thought of as a mass on two vertical springs, (one on top of the other) it is easier to understand. The upper spring being the vehicle suspension and the lower spring being the bridge, i.e. it is now a 2 degree of freedom system. The stiffness of the upper spring (the vehicle suspension) is constant. The stiffness of the lower spring (the bridge) is not constant since it depends on where the vehicle is positioned on the bridge. When the vehicle is over a bridge support the lower spring could be regarded as infinitely stiff so the vehicle behaves as an uncoupled single DOF system and the frequency remains 2.8 Hz. However, when the vehicle is at the mid-span of the bridge the lower spring is no longer infinitely stiff, as the system of springs supporting the mass is more flexible than it was before (when the vehicle was over a support) so the frequency of the system drops. Note that the 2 degree of freedom model/visualisation constitutes only an analogy that encapsulates the frequency evolution phenomena. Similar models have been reported in [25, 26] to study the dynamics of vehicle-bridge interaction systems.

Turning our attention to the upper solid line in Fig. 7, the result shows how the bridge frequency changes with respect to the position of the vehicle on the bridge. The most relevant thing about this plot is that for certain truck positions the bridge frequency is actually predicted to increase. This is counterintuitive because one would expect the bridge frequency to reduce slightly if a concentrated un-sprung mass was placed on the bridge deck. (This is indeed what would happen and this is demonstrated later in Fig. 12). However, it appears that when the moving mass is sprung, there are situations where the bridge frequency can actually increase slightly. It is conceivable that the sprung mass (truck body) adds a kind of inertial resistance to bridge’s motion. In other words, the vehicle mass is providing some restraint to the upper end of the truck suspension (spring), which is touching the bridge deck. This can be interpreted as if the truck provides an extra spring support at the location the truck is located at. Obviously, from a static point of view, the number of bridge supports remains unchanged. For convenience in this paper we will term this apparent localised stiffening of the beam where the truck is parked an ‘inertial spring support’. It can be seen in the upper solid line in Fig. 7 that when the truck is at either of the 2 short side spans the addition of this inertial spring support makes very little difference to the bridge frequency, indicating that it is adding relatively little stiffness to the system. However, when the truck is on the longer central span, the addition of an 'inertial spring support' does result in a significant increase in frequency.

Conceptualising the body of the vehicle as described above is helpful for initial visualisation as it allows the bridge to be idealised in a conventional static structural arrangement. However, in reality the vehicle-bridge system is a dynamic system so the behaviour is more complex and insight on the behaviour is provided by [5]. Using a simple numerical model of a sprung mass on a single span beam, they investigated how the system frequencies changed as the sprung mass was positioned at different points on the beam. The results of [5] showed frequency variation patterns similar to those shown in Fig. 7. Moreover, they found that the increase and decrease in bridge and vehicle frequencies respectively was sensitive to the frequency ratio (FR), where FR= vehicle frequency / bridge frequency. For systems where the vehicle frequency was less than the bridge frequency (which is the situation here) and when FR was close to one (e.g. 0.95), their model shows that large shifts in bridge and vehicle frequencies would occur. However, when FR was not close to one (e.g. 0.5) the frequency shifts predicted by the model were significantly smaller. The difference in the magnitude of the frequency shift with respect to FR shows that it is not as simple as thinking of the truck mass as a restraint. It appears that the closer the vehicle frequency is to the bridge frequency the more pronounced this restraint is, which demonstrates the dynamic nature of the restraint. It was also shown in [5] that the frequency shifts predicted by the model were larger for higher mass ratios (MR) where MR=vehicle mass / bridge mass.

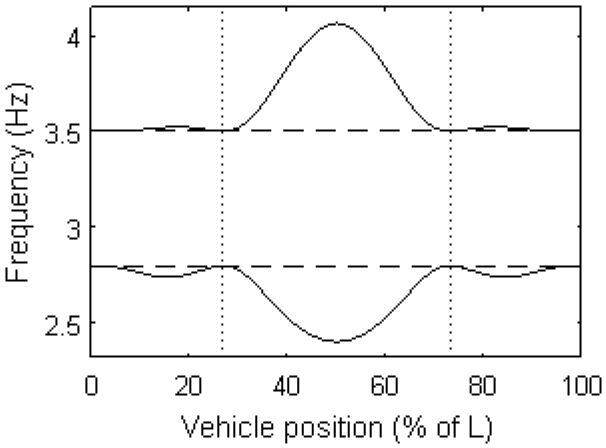

Fig. 7: Numerical frequency evolution of uncoupled system (dashed lines) and coupled system (solid lines). Vertical dotted lines indicate intermediate bridge supports.

Although the numerical model used to generate Fig. 7 is only an approximation of the real bridge, it does clearly show that the frequency content during a vehicle passage is likely to change. This variation in frequency with respect to vehicle position makes the problem non-stationary and the acceleration signals recorded during the passage of the vehicle should reflect the non-stationary nature of the process, i.e. a change in frequency should be evident. To examine if this frequency change is evident, the acceleration response from centre of span 3 (sensor C in Fig. 4) is analysed using the wavelet approach described in Section 2.3. Fig. 8(a) shows the acceleration time series recorded at sensor C during a truck passing event. For this crossing event the first axle of the truck enters the bridge at 6 s and the last axle exits the bridge at 26 s. The truck entering and leaving the bridge is indicated in the figure by dotted vertical lines. Thus, the signal between these two lines corresponds to forced vibration data, whereas the acceleration after the truck leaves is the free vibration data. Fig. 8(b) shows the conventional wavelet transform of the complete time series shown in Fig. 8(a) and Fig. 8(c) shows the wavelet coefficients after calculating the envelope along scales and normalizing by instantaneous energy (see Section 2.3). In Fig. 8(b) & (c) the truck entering and leaving the bridge is again indicated using dotted vertical lines. Parts (b) and (c) of the figure also have dashed horizontal lines at 3.5 Hz and 2.8 Hz. The dashed horizontal line at 3.5 Hz is the uncoupled bridge frequency and the dashed horizontal line at 2.8 Hz is believed to be the approximate uncoupled vehicle frequency. In the absence of a modal test on the vehicle, one cannot say definitively that 2.8 Hz is the vehicle frequency, but based on the numerical model and the available experimental data the authors believe this is a reasonable supposition. The conventional CWT result (Fig. 8(b)) shows only some high energy concentration within the studied frequency range when the vehicle is traversing the middle span. On the other hand, the processed wavelet coefficients (Fig. 8(c)) provide a better picture of the relative energy distribution in the time-frequency plane. The frequency evolution is not entirely clear in the CWT plot in Fig. 8(c). However, it is apparent that during free vibration the bridge is vibrating only at its fundamental frequency (3.5 Hz) as all the energy is concentrated there. On the other hand when the truck is on the bridge (forced vibration) there is also a significant amount of energy near what the authors believe to be the vehicle's first frequency (2.8 Hz). Furthermore, a trend seems to be evident in Fig. 8(c) similar to the one predicted Fig. 7. During the period 12-20 s when the vehicle is crossing the central span of the bridge the vehicle frequency seems to go down and the bridge frequency seems to go up.

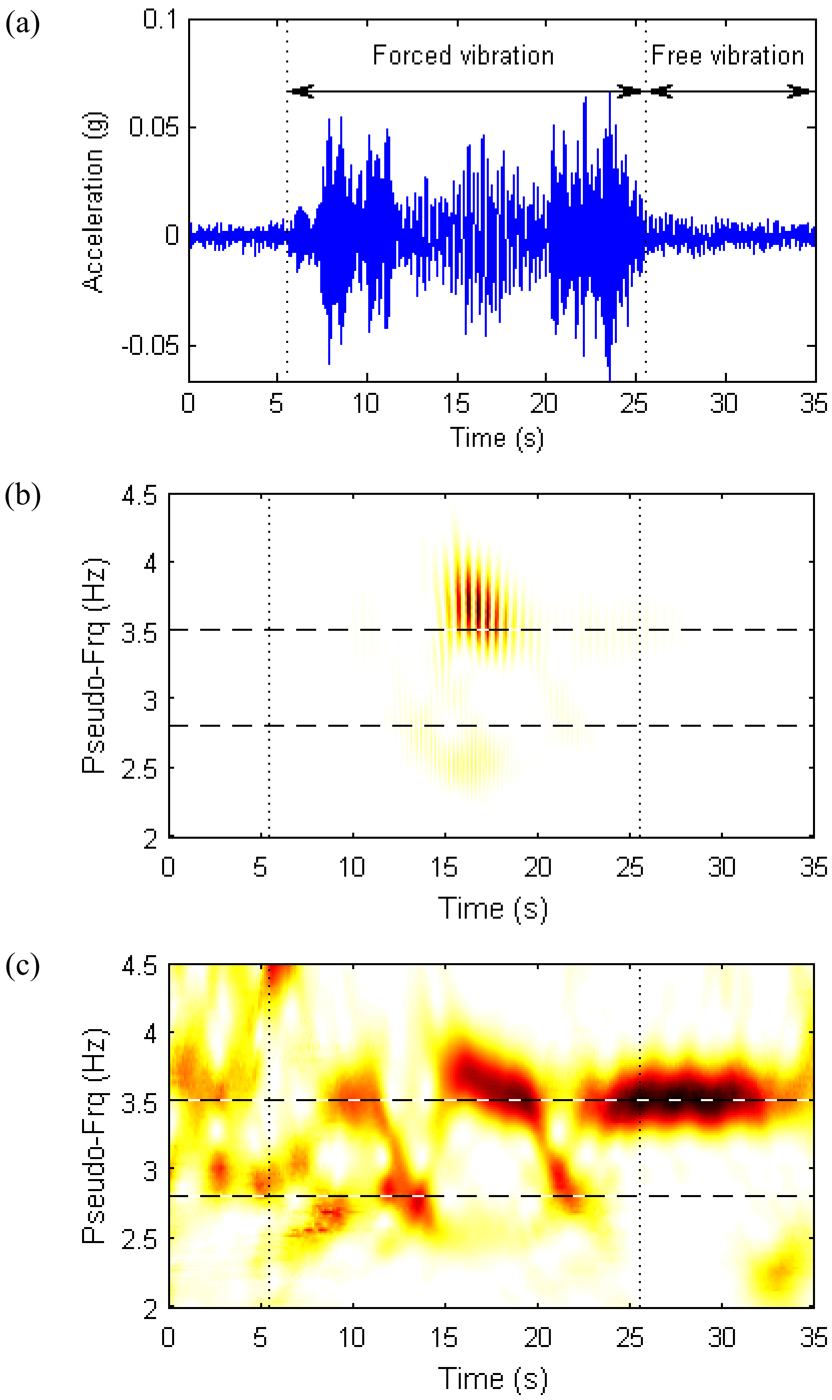

Fig. 8: Acceleration and frequency content for truck passage on Bridge A (a) Acceleration signal; (b) Raw CWT result; (c) Processed CWT; Vertical lines = start/end of forced vibration; Horizontal dashed lines = uncoupled system frequencies

Although Fig. 8 partially supports the theoretical construct presented in Fig. 7, it is difficult to draw any firm conclusions about the validity of the suggested explanations. This is because the frequencies presented in Fig. 7 are calculated for the vehicle model being situated at a series of discrete locations on the beam. Unfortunately, the experimental data in this section is for a moving truck and it could justifiably be argued that it is not correct to apply FDD to a non-stationary process to extract the modal properties. Therefore, it is not possible to reliably extract the modes of the coupled system while the vehicle is moving. This means that the frequency peaks shown in Fig. 6 are likely to be a good approximation of the real frequencies but will not be totally accurate. To overcome these issues a new experiment, where a truck is parked at a series of discrete locations on a bridge, is undertaken and this work is reported in the next section.

4. Experimental study of Bridge B and stationary truck

As explained at the end of the previous section the experimental results from Bridge A cannot really be used to check the validity of the concept presented in Fig. 7. In the previous experiment the truck was moving, but in the numerical model the truck was parked at a series of discrete locations. To resolve this issue a second experimental campaign was undertaken where a truck was actually parked at a number of discrete locations on the bridge and the results are described herein. To make sure that the bridge behaviour observed in Section 3 was not specifically related to Bridge A or the test truck shown in Fig. 3(b), in this next experiment a different bridge and truck are used. It is important to note that when a vehicle is parked on the bridge the system is coupled but stationary, i.e. the modal parameters will remain constant. Therefore, using output-only modal analysis techniques such as FDD to extract the modal properties is appropriate.

4.1 Bridge and instrumentation description

A photo of the bridge used in this experiment is shown in Fig. 9(a) and a plan view in Fig. 10(a). The bridge is a half through steel girder bridge, it spans 36 m and the deck is simply supported. The 7.6 m wide, and 200 mm deep concrete deck is supported on a series of 450 mm deep steel beams, which span transversely between the main girders which are approximately 2 m deep. As explained in Section 3.1, for experiments of this type, a high vehicle-bridge mass ratio is desirable, so a light bridge deck is advantageous. The reason for choosing this bridge is that the deck is light compared to other bridges of the same span, i.e. the primary members are steel and the deck is relatively narrow. Again with the objective of having a high (vehicle-bridge) mass ratio, the truck selected for this test had a total weight of

32 tonnes, which is heavier than the 26 tonnes truck used in the previous test. The test truck used has four axles and is shown in Fig. 9(b). While the bridge was chosen for its technical advantages described above, logistically the disadvantage of the bridge was that it was in an urban area and frequently trafficked, which made finding a quiet time to carry out the test challenging.

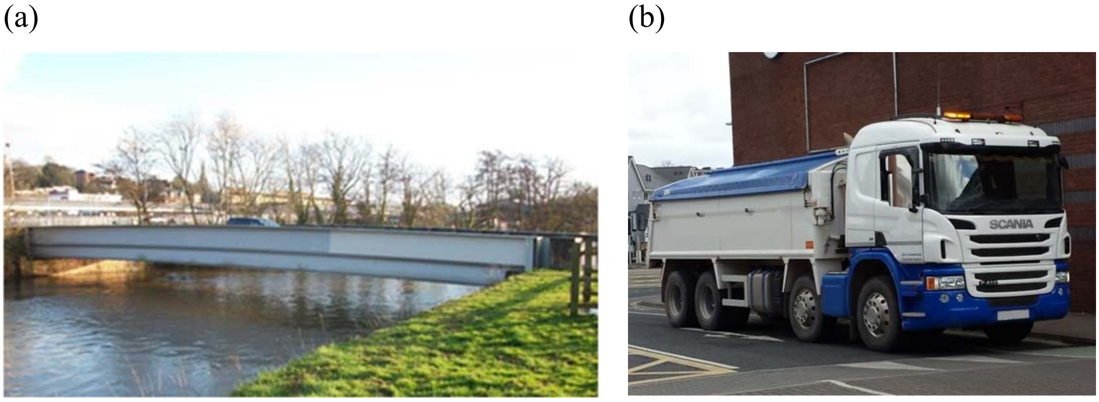

Fig. 9: (a) Bridge B elevation; (b) Test truck

The instrumentation used in this experiment consisted of four accelerometers attached to the main girders. The position of the four accelerometers (A-D) is shown in Fig. 10(a). The accelerometers used in this test were Honeywell QA750 force balance accelerometers and the scanning frequency used was 128 Hz. Fig. 10(b) shows accelerometer B attached to the underside of the top flange of the main girder via a magnet. The vehicle was parked for short durations at ¼-span, mid-span and ¾-span. A full bridge closure was not permitted so the test was carried out early in the morning when there was little traffic. Ideally, the truck would stay parked at a given location for as long as possible, because the longer the time series the more accurate the subsequent modal analysis is likely to be. However, the fact there was no bridge closure meant that the stops had to be kept relatively short. Only stop durations of 10-12 s were feasible. However, signals of this length are sufficiently long to allow the modal properties to be determined accurately.

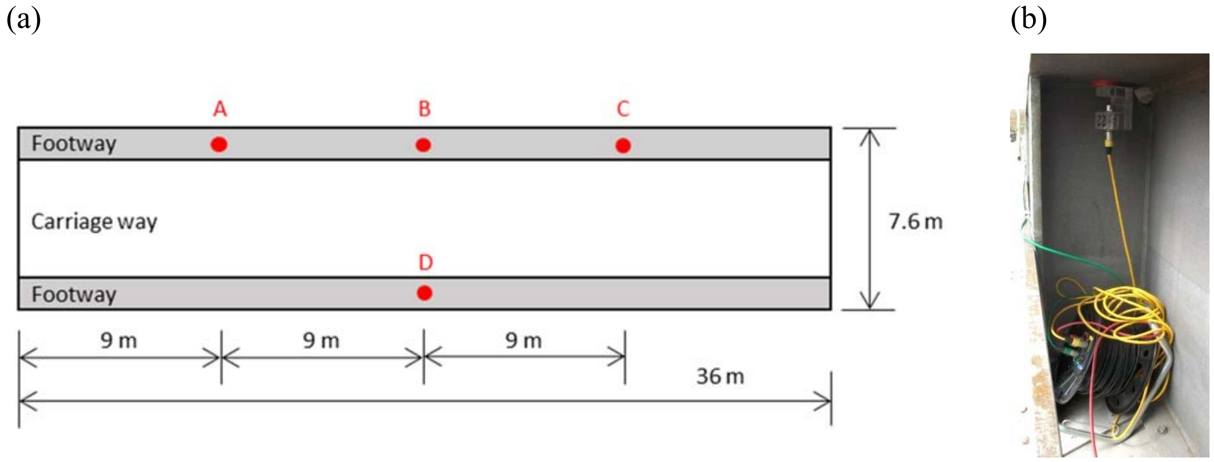

Fig. 10: Dimensions and instrumentation details for Bridge B (a) Plan view of bridge deck and sensor locations; (b) Accelerometer attached to underside of the girder top flange.

4.2 Evolution of Vehicle-Bridge system

Analysing the ambient vibration data, the fundamental (first bending) frequency of the bridge was identified as 3.13 Hz. Fig. 11(a) shows the time series recorded at accelerometer B for a full set of truck movements, namely; truck coming on to the bridge, parking at ¼-span, moving on and parking at mid-span, then finally moving to ¾-span and parking briefly before exiting the bridge. The different portions of the signal are demarcated using vertical dotted lines and the parts of the signal corresponding to the truck being parked at particular locations on the bridge can be identified using the annotations on the bottom of the figure. The annotations on the top of the figure have been added to allow the reader visualise what the truck is doing for each section of the signal. For the first 25 seconds the bridge is in ambient vibration (A). Then the truck moves (TM) on to the bridge arriving at the ¼-span at approximately 35 s. On arrival at ¼-span the truck stops and remains there for approximately 12 seconds and this section of the signal is termed ‘loaded free vibration (LF)’. TM and LF are repeated in sequence so that the truck can be parked for a short duration at mid-span and ¾-span. When the truck leaves the bridge, the bridge is in free vibration (F). For the data presented in Fig. 11 the only vehicle on the bridge was the test truck, i.e. there was no other traffic crossing the bridge. Much of the bridge vibration evident in the figure is believed to be due to the energy input into the bridge during the four truck movements..

To observe how the bridge frequency evolves over the course of the truck movements, the time series in Fig. 11(a) is analysed using CWT, and the results are presented in Fig. 11(b).

Again, the vertical dotted lines demarcate the different parts of the signal (i.e. the lines correspond to those shown in part (a) of the figure) and it can be seen that during ambient vibration at the start of the signal the bridge vibrates predominantly at its unloaded fundamental frequency (3.13 Hz) with no significant energy at any other frequency. The same is true for the free vibration at the end of the signal. During the four truck movement phases (TM) there is no clear pattern of the energy distribution in the time-frequency domain. However, during the loaded free vibration events (LF), the energy is concentrated along clear frequency bands. For example, when the truck is parked at mid-span (65-81 s) the energy is concentrated in two distinct bands at approximately 2.5 Hz and 3.5 Hz. Similarly, when the truck is at the ¾-point (95-105 s) it can be seen that there is significant energy at these bands with almost no energy at the fundamental frequency, indicated by the horizontal dashed line in the figure.

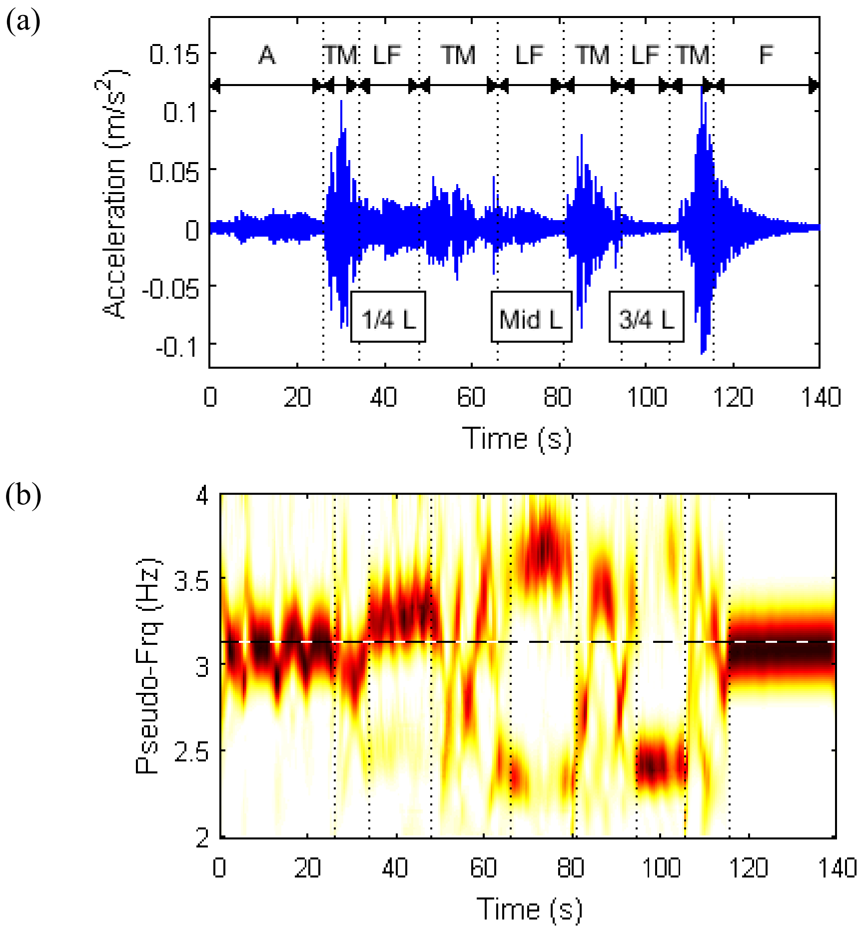

Fig. 11: Experimental data from Bridge B; (a) acceleration signal recorded at mid-span during a series of truck movements; (b) CWT of acceleration signal; Vertical lines = start/end of forcing regime; Horizontal dashed lines = bridge's fundamental frequencies

While the CWT plot shown in Fig. 11(b) is useful to visualise the frequency shift for the different truck positions, its frequency resolution is limited. To identify the frequencies more accurately the LF portions of the signal when the truck is at ¼-span, mid-span and ¾-span are analysed using FDD and the identified frequencies are plotted as circular data markers at 25%, 50% and 75% of L respectively, in Fig. 12. The experimental results indicate that the bridge and vehicle frequencies increase and decrease respectively when the truck is on the bridge with the largest changes occurring when the truck is in the centre of the bridge. The upper and lower (solid) lines in Fig. 12 respectively show the bridge and vehicle frequencies predicted by the numerical model described in Section 2.1, for a simply supported single span beam. In line with the modelling philosophy described in Section 3.3, the bridge properties in the model were revised so that the uncoupled bridge frequency in the model matches the experimentally observed fundamental bridge frequency (3.13 Hz). A similar approach is also used to revise vehicle properties. Based on the extracted values in Fig. 12 an uncoupled vehicle frequency in the region of 2.6 Hz seems sensible. Therefore the suspension property of the vehicle model (i.e. the spring stiffness) has been amended such that for a sprung mass of 32,000 kg the uncoupled vehicle frequency is 2.6 Hz. As the numerical model is a relatively simple, the frequencies predicted by the model do not exactly match the frequencies observed experimentally. However, the comparison highlights that the trends are the same. This is important because it demonstrates that the evolution of the system frequencies (bridge and vehicle) predicted by the model are credible. Moreover, it shows that the hypothesis put forward in Section 2.3 to explain the behaviour observed in Bridge A is also credible.

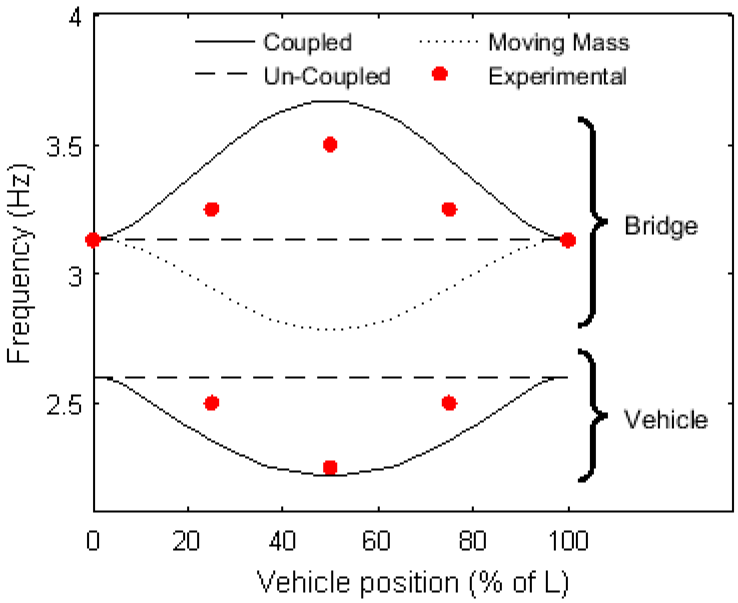

Fig. 12: Frequency evolution during vehicle passage. Solid line = Coupled system; Dashed line = uncoupled system; Dotted line = Moving mass case; Red dots = experimental values

Finally, the dotted plot in Fig. 12 shows the bridge frequency predicted by the numerical model if an un-sprung mass of 32,000 kg is placed at a series of discrete locations along the length of the bridge. The model predicts that for an un-sprung mass the bridge frequency will be reduced, with the largest reduction occurring when the mass is at the centre of the bridge. This reduction in frequency with the addition of mass is in line with what one might intuitively expect for a (sprung) truck but this is clearly not what actually occurs.

4.3 Modes of vibration

So far previous sections have focused on studying how different truck positions affect the frequencies of the vehicle-bridge system. In this section, changes in the associated mode shapes of the vehicle-bridge system are reported. To make sense of the theoretical frequency predictions presented in Fig. 7 the reader was prompted to visualise the body mass of the vehicle as supported on two springs, the upper spring representing the vehicle suspension and lower spring representing the bridge stiffness. While this is a useful analogy to visualise what is happening it is technically incorrect because the lower spring is in fact a beam. The significance of this is that when the sprung mass is on the bridge, the frequency that we have been referring to up to now as the vehicle frequency will have a mode associated with it that includes the deformed shape of the beam.

Up to now this paper has talked about ‘vehicle’ frequency and ‘bridge’ frequency because based on conventional thinking it is the most straightforward way to explain the experimental results that have been reported so far. However, to understand the modes associated with the observed frequencies it is important to appreciate that as soon as the vehicle is on the bridge, the vehicle and the bridge behave as one system, not two independent systems. Therefore, technically it is not appropriate to talk about vehicle and bridge modes, it would be more correct to talk about the coupled system’s first and second mode. However, for simplicity and convention, when presenting the relevant modes below they will still be referred to as ‘vehicle mode’ and ‘bridge mode’ even though it is not totally correct.

The easiest way to appreciate the mode of vibration of the coupled system is to examine the modes predicted by the numerical model. In particular, Fig. 13 shows the modes of vibration for three different vehicle locations; (i) over the left support, (ii) ¼-span and (iii) mid-span. The eigenvalue analysis of the coupled system is carried out and modal ordinates of the degrees of freedom of the vehicle and bridge can easily be computed. When the vehicle is at the bridge’s left support, both systems are effectively uncoupled and the familiar (independent) modes for the vehicle (Fig. 13(a)) and bridge (Fig. 13(b)) are observed. In particular note how the bridge part of the ‘vehicle mode’ (Fig. 13(a)) remains straight. However, when the vehicle is at ¼-span the bridge clearly plays a role in the ‘vehicle mode’ as the bridge is now in a curved shape (see Fig. 13(c)). Interestingly when the vehicle is at ¼-span the deformed shape of the bridge is approximately similar for both the ‘vehicle mode’ (Fig. 13(c)), and the ‘bridge mode’ (Fig. 13(d)). A similar pattern is observed when the vehicle is at mid-span Figs. 13 (e) and (f).

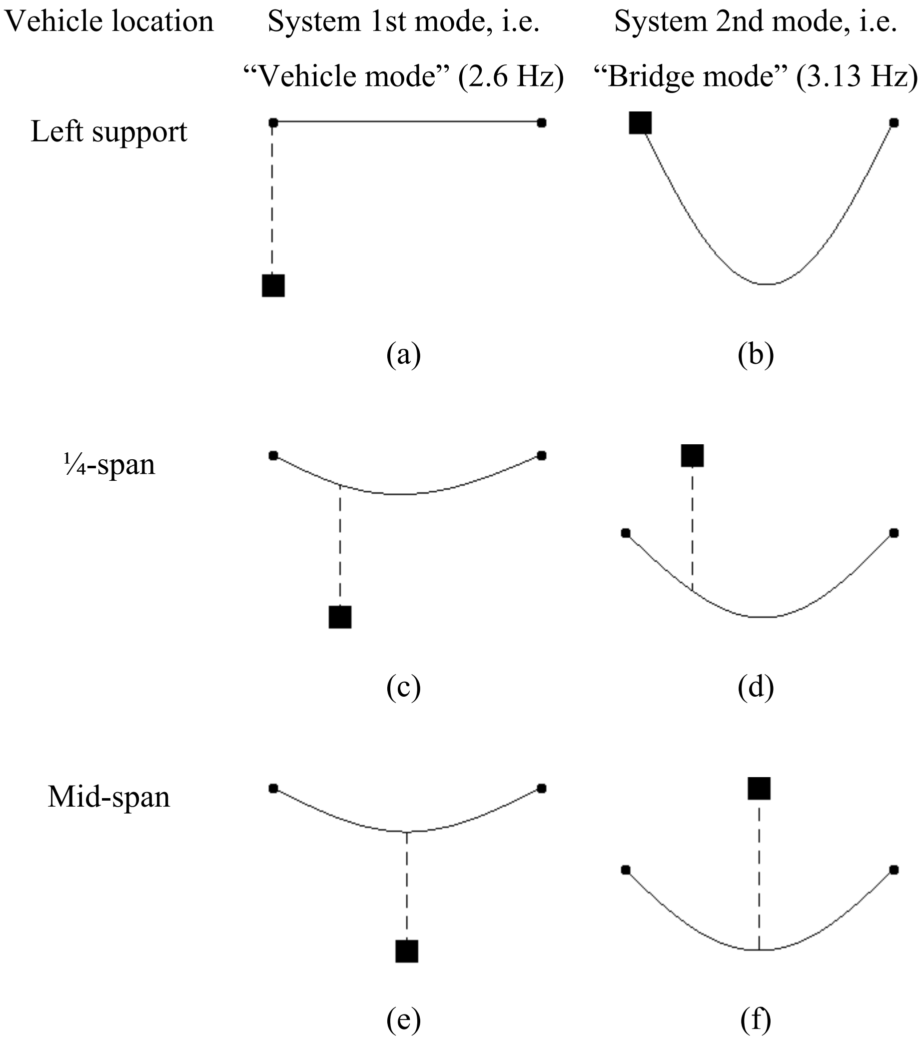

Fig. 13: Numerical mode evolution for coupled system

It should be noted that the modes of vibration plotted in Fig. 13 are schematic in nature. Their primary purpose is to demonstrate that when the vehicle is on the bridge the system is coupled. The resulting modes can be more usefully thought of as the system's 1^{st} and 2^{nd} modes. To examine in more detail how the bridge part of the full system modes of vibration vary with truck position, just the bridge part of the 1^{st} and 2^{nd} system modes are plotted in Fig. 14. Since no acceleration was measured on the vehicle, only the bridge part of the mode can be examined in detail. Parts (a), (b) and (c), (d) of Fig. 14 are generated using the numeric model and experimental data respectively. The bridge part of the system 1^{st} mode ('vehicle mode') predicted by the numerical model for three different truck positions (¼-span, mid-span, and ¾-span) are plotted in Fig. 14(a). In the figure it can be seen that the bridge part of the 'vehicle mode' has three distinct shapes for the three different truck locations considered. When the truck is at ¼-span the bridge part of the mode is slightly skewed to the left, for the ¾-span position it is skewed to the right and when the vehicle is at mid-span it is symmetric. Fig. 14(c) shows the equivalent modal ordinates obtained experimentally and for the three test points. Admittedly as the experiment only provides three modal ordinates it is not possible to make definitive comment on whether the mode shapes are skewed or not. However, for the three modal ordinates available, we can observe that they are behaving in a manner consistent with the equivalent location of the theoretical mode shapes shown in Fig. 14(a).

Fig. 14(b) shows the bridge part of the system 2nd mode (‘bridge mode’) predicted by the numerical model for three different truck positions. It can be seen in the figure that the bridge part of the system 2nd mode does not change significantly with vehicle position but there is some small variation. Essentially, the numerical model indicates that the bridge part of the mode is slightly skewed to the opposite side of where the vehicle is located. The equivalent experimental modal ordinates are plotted in Fig. 14(d). Similar to Fig. 14(c), in Fig. 14(d) only three modal ordinates are available and therefore there is insufficient evidence to determine if the subtle skewing of modes evident in Fig. 14(b) is also present experimentally. However, it can be said that the magnitude of the modal ordinates at a given location are quite similar for all three truck positions. This is consistent with the theoretical modes presented in Fig. 14(b) which as mentioned previously appear relatively insensitive to vehicle position. Note that all the plots in Fig. 14 have been normalized to have a minimum value of -1 at mid-span for ease of comparison.

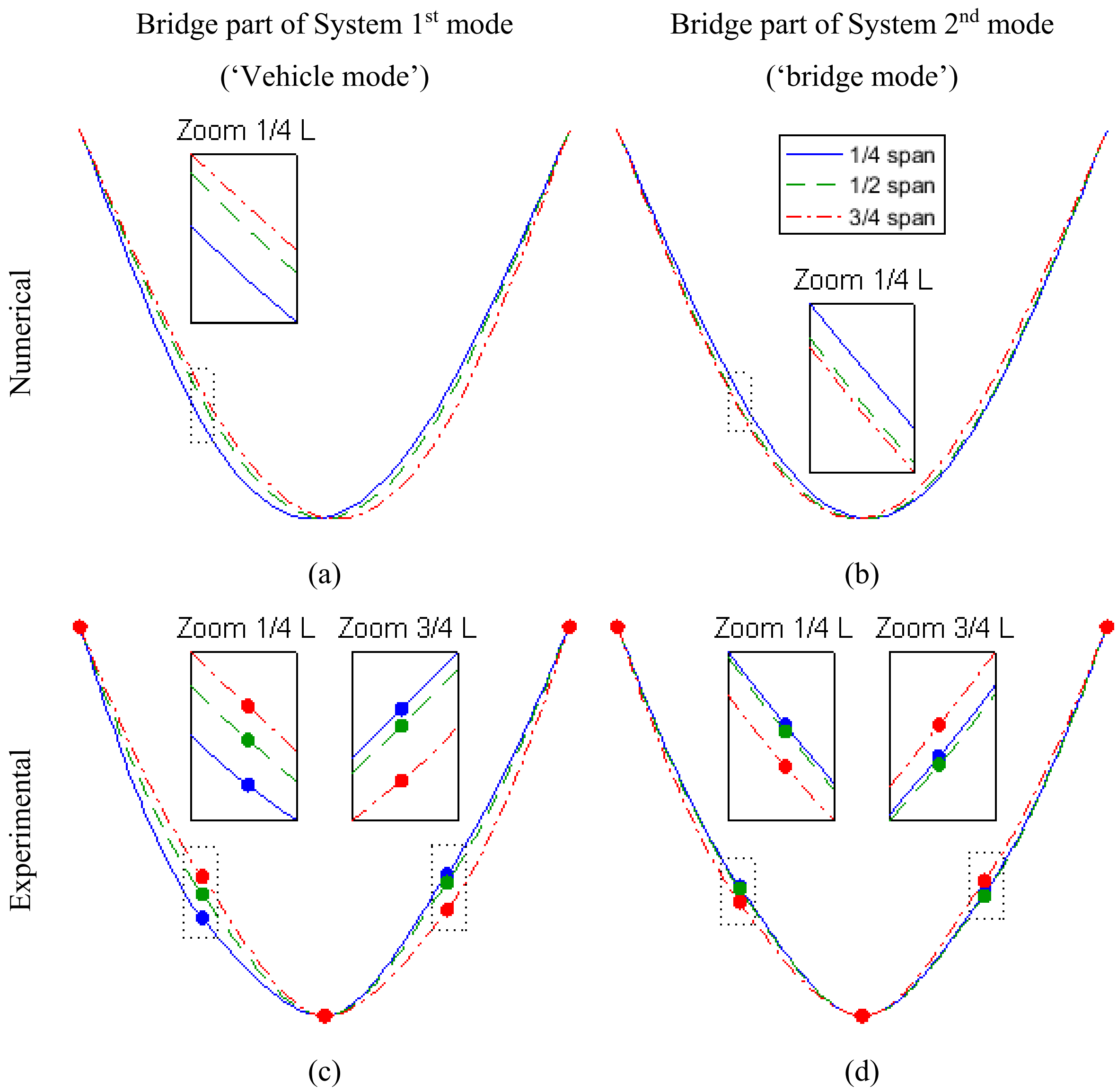

Fig. 14: Bridge part of system 1st and 2nd modes for different truck positions (a) 1st mode calculated theoretically, (b) 2nd mode calculated theoretically, (c) 1st mode measured experimentally, (d) 2nd mode measured experimentally.

5. Conclusions

This paper investigated the changes in frequencies and modes of vibration of a vehicle-bridge system. Two different bridges A and B were studied. Initial experimental results observed on bridge A included some unexpected behaviour. In particular when the truck was on the bridge the fundamental bridge frequency seemed to increase and a frequency peak not present in free vibration appeared on the spectrum. This prompted the development of a numerical model to try and provide a theoretical explanation for the observed behaviour. The model provided a theoretical framework which seemed to explain the observed behaviour. However, to further investigate the phenomena a second experiment was carried out where the truck parked at a series of discrete locations on the bridge. This experiment was carried out on Bridge B and, by using time-frequency analysis and output-only modal analysis, the unexpected behaviour was further clarified.

Furthermore, in the course of the investigation a number of interesting observations were made. For example, a coupled vehicle-bridge system might feature significant changes in natural frequencies depending on the vehicle's position. Also when analysing forced vibration signals the presence of additional frequencies on the spectrum proves system coupling. Moreover, it is shown numerically and experimentally, that the modes of vibration of the coupled system do change with the location of the vehicle. However, the amount of change differs for the 'vehicle' and the 'bridge' modes. In particular, it is shown that when the vehicle is on the bridge the 'vehicle' mode has a significant 'bridge part' associated with it and the shape of this part is very similar to the bridge's fundamental mode of vibration.

Numeric models indicate the magnitude of the changes in modal parameters will be more pronounced for situations with high vehicle-bridge mass ratios. However, this paper shows that it is a reality for conventional heavy vehicles and relatively light standard bridges.

Acknowledgements

The research leading to these results has received funding from the People Programme (Marie Curie Actions) of the European Union's Seventh Framework Programme (FP7/2007-2013) under grant agreement n° 330195. The authors would also like to thank John Vittery of EM Highways Services Limited, and the Bridge Section of The Engineering Design Group of Devon County Council led by Kevin Dentith BSc, CEng, FICE, for their support and assistance with this work.

References

[1] E.B. Magrab, Vibrations of Elastic Systems – With Applications to MEMS and NEMS, Springer, Dordrecht, 2012.

[2] L. Frýba, Vibration of Solids and Structures under Moving Loads, third ed., Thomas Telford, Prague, 1999.

[3] Y.B. Yang, M.C. Cheng, K.C. Chang, Frequency variation in vehicle-bridge interaction systems, Int. J. Struct. Stab. Dyn. 13 (2013) 1-22.

[4] J. Li; M. Su; and L. Fan, Natural frequency of railway girder bridges under vehicle loads, J. Bridge Eng. 8 (2003) 199-203.

[5] D. Cantero, E.J. OBrien, The non-stationarity of apparent bridge natural frequencies during vehicle crossing events, FME Trans. 41 (2013) 279-284.

[6] K.C. Chang, C.W. Kim, S. Borjigin, Variability in bridge frequency induced by a parked vehicle, Smart Struct. Syst. 13 (2014) 755-773.

[7] M.D. Spiridonakos, S.D. Fassois, Parametric identification of time-varying structure based on vector vibration response measurements, Mech. Syst. Sig. Process. 23 (2009) 2029-2048.

[8] C.Y. Kim, D.S. Jung, N.S. Kim, S.D. Kwon, M.Q. Feng, Effect of vehicle weight on natural frequencies of bridges measured from traffic-induced vibration. Earthquake Eng. Eng. Vibr. 2 (2003) 109-115.

[9] F. Xiao, G.S. Chen, J.Leroy Hulsey, W. Zatar, Characterization of non-stationary properties of vehicle-bridge response for structural health monitoring, Adv. Mech. Eng. 9 (2017) 1-6.

[10] C.C. Caprani, E. Ahmadi, Formulation of human–structure interaction system models for vertical vibration, J. Sound Vib. 377 (2016) 346-367.

[11] X. Kong, C.S. Cai, B. Kong, Numerically extracting bridge modal properties from dynamic responses of moving vehicles, ASCE J. Eng. Mech. 142 (2016) 1-12

[12] E.J. OBrien, A. Malekjafarian. A mode shape-based damage detection approach using laser measurement from a vehicle crossing a simply supported bridge, Struct. Control Health Monit. 23 (2016) 1273-1286.

[13] D.M. Siringoringo, Y. Fujino, Estimating bridge fundamental frequency from vibration response of instrumented passing vehicle: analytical and experimental study, Adv. Struct. Eng. 15 (2012) 417-433.

[14] Matlab, MathWorks, 2013.

[15] O.C. Zienkiewicz, R.L. Taylor, The Finite Element Method – Volume 1: The Basis, fifth ed., Butterworth Heinemann, Oxford, 2000.

[16] P. Lou. Finite element analysis of train-track-bridge interaction system, Arch. Appl. Mech. 77 (2007) 707-728.

[17] Y.B. Yang, J.D. Yau, Y.S. Wu, Vehicle-Bridge Interaction Dynamics – With Applications to High-Speed Railways, World Scientific, Singapore, 2004.

[18] L. Gyenes, C.G.B. Mitchell, S.D. Phillips, Dynamic pavement loads and tests of road-friendliness for heavy vehicle suspensions, in: D. Cebon, C.G.B. Mitchell (Eds.), Heavy Vehicles and Roads: Technology, Safety and Policy, Thomas Telford, London, 1992, pp. 243-251.

[19] D.J. Ewins, Modal Testing. Theory, Practice and Application. second ed., Research Studies Press LTD, Baldock, 2000.

[20] C. Rainieri, G. Fabbrocino, Operational Modal Analysis of Civil Engineering Structures. An Introduction and Guide for Applications, Springer, New York, 2014.

[21] A. Cohen, R.D. Ryan, Wavelets and Multiscale Signal Processing, Chapman & Hall, London, 1995.

[22] S.G. Mallat, A Wavelet Tour of Signal Processing, second ed., Academic Press, London, 1999.

[23] D. Cantero, M. Ülker-Kaustell, R. Karoumi. Time–frequency analysis of railway bridge response in forced vibration, Mech. Syst. Sig. Process. 76-77 (2016) 518–530.

[24] Y.B. Yang, C.W. Lin, J.D. Yau, Extracting bridge frequencies from the dynamic response of passing vehicle. J. Sound Vib. 2072 (2004) 471-493.

[25] R. Cantieni, Investigation of vehicle-bridge interaction for highway bridges. In: Heavy Vehicles and Roads: Technology, Safety and Policy, Thomas Telford, London, 1992.

[26] H. Ludescher, E. Brühwiler, Dynamic amplification of traffic loads on road bridges, Struct. Eng. Int. 19 (2009) 190-197.